

# Belief-Adaptive MAP Detection for Molecular ISI Channels with Heteroscedastic Noise

Erencem Ozbey, H. Birkan Yilmaz, and Chan-Byoung Chae

**Abstract**—Inter-symbol interference (ISI) with heteroscedastic, or state-dependent, noise is a defining feature of molecular communication via diffusion (MCvD). However, such noise variance dependency across ISI states has not been systematically considered in prior detector designs. This letter introduces two decoding mechanisms, Belief-Adaptive Maximum A Posteriori (BA-MAP) and Soft BA-MAP, that explicitly incorporate state-dependent means and variances of the molecular count channel. The BA-MAP method derives per-symbol adaptive MAP thresholds based on the receiver’s current state beliefs, whereas the Soft BA-MAP approach computes mixture log-likelihood ratios by weighting all possible ISI states. Simulation and information-theoretic analyses confirm that the proposed detectors outperform conventional equalization and fixed-threshold methods, achieving up to 100% throughput improvement under realistic MCvD settings.

**Index Terms**—Inter-Symbol Interference, Molecular Communications, Information Rate.

## I. INTRODUCTION

**M**OLECULAR communication is a paradigm in which molecules are used as information carriers instead of electromagnetic waves or electrical signals [1], [2]. Inspired by biological systems, molecular communication via diffusion (MCvD) encodes information into molecules that are released into a diffusive medium by a transmitter (Tx) node to convey information through chemical signals. Through the diffusion process, the receiver (Rx) detects these molecules and decodes the transmitted information [3].

In general, MCvD systems operate with discrete and fixed-duration symbol intervals. However, due to the long diffusive tail, molecules released during one interval may continue to arrive in several subsequent intervals, leading to severe inter-symbol interference (ISI). Several modulation techniques have been proposed to mitigate ISI at the system level. For example, Molecular Shift Keying (MoSK) [4], where the transmitter emits different types of molecules, and Zebra-CSK [5], which uses inhibitors to destroy molecules in the environment, are modulation-level approaches designed to reduce ISI.

A modulation scheme defines how information is encoded in one or more properties of molecular signals (e.g., molecule type, concentration, or release timing), which in turn influences the effective channel impulse response. However, the impulse response itself does not solely determine communication performance; reliable transmission ultimately depends on the detection strategy employed at the receiver [6]. In MCvD

systems, the received signal is generally represented by the number of molecules observed as a function of time.

The arrival of the molecules in an interval exhibits a Binomial model [7]. Under common counting models (Poisson and Gaussian approximations), both the mean and the variance of the received molecules in an interval depend on the recent bit history [8]. Thus, the channel is a finite-state channel with memory and heteroscedastic (state-dependent) noise. Simple fixed threshold detectors disregard this memory and variance structure. In order to mitigate ISI under a modulation, one alternative can be using transmitter (Tx) side equalization techniques such as Power Adjustment (PA) [9]. On the other hand, receiver-side equalizers such as MMSE [10] reduce effective memory but typically revert to a single hard threshold after linear processing, leaving variance asymmetry underexploited for detection. A classic way to take heteroscedasticity into account is Maximum a Posteriori (MAP) sequence detection [10] by using the Viterbi [11] algorithm. However this algorithm brings a decision (traceback) delay and a need for an additional storage mechanism to save survivor paths. Blockwise iterative methods as introduced in [12] also introduce a decision delay and are not suitable for time-critical scenarios.

In this work, we propose state-dependent signal detection methods that explicitly model ISI and operate causally with zero decision delay, which do not employ a traceback:

- **BA-MAP: Belief-adaptive MAP thresholding.** To obtain a lightweight, hardware-friendly detector, we model the state uncertainty into belief-matched Gaussian models and select the threshold  $\tau$  by the MAP condition.
- **Soft BA-MAP: Soft-belief, mixture MAP-LLR detection.** The Rx maintains a soft belief (a probability distribution) over ISI states. For each observation, it evaluates the posterior odds of bit-1 versus bit-0 using belief-weighted Gaussian mixtures and decides by the sign of the log-likelihood ratio (LLR). This rule is Bayes-optimal for symbol-wise detection given the current state beliefs, minimizes the per-bit error probability, and naturally incorporates unequal priors.

For evaluating these methods, we develop an information-rate estimator, providing a theoretical analysis of how ISI and state-dependent processing impact fundamental throughput.

*Contributions:*

- 1) We formulate the finite-state, heteroscedastic channel and derive a belief-driven *mixture MAP-LLR* detector (Soft BA-MAP) that utilizes the full state mixture.
- 2) We develop a *belief-adaptive MAP threshold* (BA-MAP) that retains state awareness.
- 3) We provide an information-rate framework and analyze the maximum achievable rates of these strategies.

E. Ozbey and H. B. Yilmaz are with NETLAB, Department of Computer Engineering, Bogazici University, Istanbul, Turkiye. (e-mails:ozbeyerencem@gmail.com; birkan.yilmaz@bogazici.edu.tr)

C.-B. Chae is with the School of Integrated Technology, Yonsei University, Seoul 03722 Korea (e-mail: cbchae@yonsei.ac.kr)

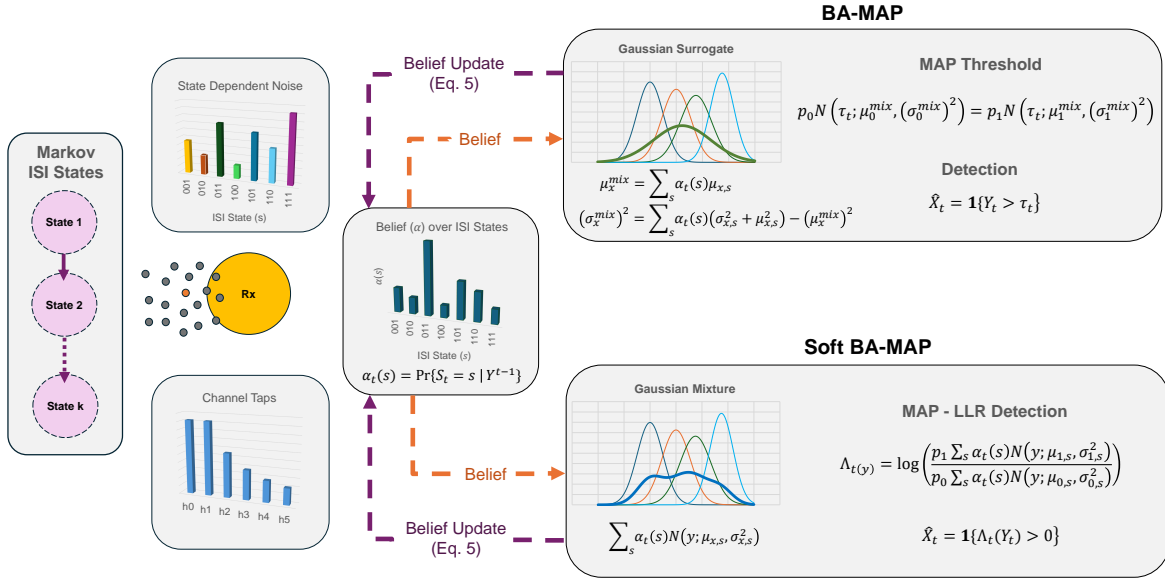


Fig. 1. Belief-adaptive detection for molecular ISI channels with state-dependent noise. The MCvD channel is modeled as a finite-state ISI channel whose received-count statistics depend on the ISI state. The receiver maintains a causal belief over ISI states via forward recursion, and uses this belief to adapt detection. Soft BA-MAP performs symbol-wise MAP detection using belief-weighted Gaussian-mixture likelihoods, whereas BA-MAP reduces the mixture to a single belief-adaptive Gaussian surrogate via moment matching and applies a lightweight MAP threshold rule.

## II. SYSTEM MODEL

We work on an MCvD system where communication proceeds in symbol intervals of duration  $T_s$ . For our channel formulation,  $X_t \in \{0, 1\}$  denotes the  $t$ -th symbol with prior  $\Pr\{X_t = x\} = p_x$ , i.e.,  $p_0$  represents the probability of sending bit-0. At the Tx side when  $X_t = 1$ , the Tx releases  $N^{\text{Tx}}$  molecules at the start of interval  $t$ ; when  $X_t = 0$ , it releases none. Hence, we are considering basic On-Off Keying for the modulation part. The number of absorbed molecules by the Rx in the same symbol duration is denoted as  $Y_t$ .

Molecules from emissions in previous intervals arrive over multiple future intervals. When the ISI memory order is  $m$ , we model the signal with  $K = m+1$  taps:

$$h_k \triangleq F_{\text{hit}}((k+1)T_s) - F_{\text{hit}}(kT_s), \quad k = 0, 1, \dots, m. \quad (1)$$

which are the per-molecule arrival fractions in each symbol window. The corresponding per-molecule variance factors are

$$v_k \in \begin{cases} h_k, & \text{(Poisson counting approximation)} \\ h_k(1 - h_k), & \text{(Binomial counting).} \end{cases}$$

In practice, the ISI memory order  $m$  is chosen to realistically capture the channel response. In our experiments,  $m$  is selected such that the cumulative arrival fraction of the taps accounts for at least 70% of the total ISI memory.

Conditioned on the recent  $m+1$  bits  $(X_t, \dots, X_{t-m})$ , the count  $Y_t$  is modeled as

$$\mu_t = N^{\text{Tx}} \sum_{k=0}^m h_k X_{t-k}, \quad (2)$$

$$\sigma_t^2 = N^{\text{Tx}} \sum_{k=0}^m v_k X_{t-k}, \quad (3)$$

For each symbol,  $Y_t$  is the sum of many independent Bernoulli trials contributed by both the current and past releases. When the expected molecule count is moderate, the Central Limit Theorem justifies approximating  $Y_t$  as Gaussian

$$Y_t \sim \mathcal{N}(\mu_t, \sigma_t^2).$$

We define an ISI state as the  $m$ -bit history  $S_t = (X_{t-1}, \dots, X_{t-m}) \in \{0, 1\}^m$ . The state space has  $S = 2^m$  elements and a deterministic next-state function  $\text{next}[s, x]$ . For each  $(x, s)$  we precompute

$$\begin{aligned} \mu_{x,s} &= N^{\text{Tx}} \left( h_0 x + \sum_{k=1}^m h_k b_k(s) \right), \\ \sigma_{x,s}^2 &= N^{\text{Tx}} \left( v_0 x + \sum_{k=1}^m v_k b_k(s) \right), \end{aligned} \quad (4)$$

where  $b_k(s) \in \{0, 1\}$  is the  $k$ -th bit of state  $s$ . Since we assume  $Y_t$  is a Gaussian with state and input dependent mean/variance,

$$Y_t | (X_t=x, S_t=s) \sim \mathcal{N}(\mu_{x,s}, \sigma_{x,s}^2).$$

## III. PRELIMINARIES: INFORMATION RATE

Since Shannon's classical mutual information applies only to memoryless channels, information-theoretic analyses of MCvD channels require evaluating the information rate, which accounts for channel memory [13], [14].

$$R \triangleq \lim_{n \rightarrow \infty} \frac{1}{n} I(X^n; Y^n),$$

where  $X^n = (X_1, \dots, X_n)$  and  $Y^n = (Y_1, \dots, Y_n)$ . In MCvD channels, closed-form expressions for  $R$  are generally unavailable due to channel memory and state-dependent noise; therefore, we employ a finite-state model with a simulation-based estimator. For stationary inputs on finite-state channels,

the information rate can be expressed via information density [15]. Specifically, the authors in [15] defines the (block) information density as (p. 1148)

$$i(X^n; Y^n) \triangleq \log_2 \frac{P_{Y^n|X^n}(Y^n|X^n)}{P_{Y^n}(Y^n)}.$$

Applying the chain rule gives

$$i(X^n; Y^n) = \sum_{t=1}^n \log_2 \frac{P(Y_t | X^t, Y^{t-1})}{P(Y_t | Y^{t-1})}.$$

In our finite-state model, the state evolves deterministically as  $S_{t+1} = \text{nxt}(S_t, X_t)$  with  $S_t = (X_{t-1}, \dots, X_{t-m})$ , and the channel is conditionally memoryless given  $(S_t, X_t)$ . Therefore,  $P(Y_t | X^t, Y^{t-1}) = f(Y_t | S_t, X_t)$ , where  $f(Y_t | S_t, X_t)$  is the channel output density. By writing  $p(Y_t | \mathcal{F}_{t-1}) \triangleq P(Y_t | Y^{t-1})$ , we obtain the per-symbol information density increment:

$$i_t \triangleq \log_2 \frac{f(y_t | S_t, X_t)}{p(y_t | \mathcal{F}_{t-1})}.$$

Consequently,  $R = \lim_{n \rightarrow \infty} \frac{1}{n} \sum_{t=1}^n i_t$  is the information rate. The predictive density is a mixture over the current belief (forward state distribution)  $\alpha_t(s) = \Pr\{S_t=s | Y^{t-1}\}$ :

$$p(y_t | \mathcal{F}_{t-1}) = \sum_s \alpha_t(s) [p_0 f(y_t | s, 0) + p_1 f(y_t | s, 1)].$$

The belief is updated causally via the standard forward recursion [16] followed by normalization:

$$\alpha_{t+1}(s') \propto \sum_s \alpha_t(s) \left[ p_0 f(y_t | s, 0) \mathbf{1}\{s' = \text{nxt}(s, 0)\} + p_1 f(y_t | s, 1) \mathbf{1}\{s' = \text{nxt}(s, 1)\} \right]. \quad (5)$$

A consistent Monte Carlo estimator of  $R = I(X; Y)$  is obtained by simulating  $(X_t, S_t, Y_t)$  from the model, maintaining  $\alpha_t$ , and accumulating

$$\hat{R}_n = \frac{1}{n} \sum_{t=1}^n \left[ \log_2 f(Y_t | S_t, X_t) - \log_2 A \right], \quad (6)$$

$$A = \sum_s \alpha_t(s) (p_0 f(Y_t | s, 0) + p_1 f(Y_t | s, 1)).$$

#### IV. METHODOLOGY

This section details the state-aware mechanisms proposed in this work. Both methods operate on the channel described in Section II, with the set of precomputed per-state means/variances  $\{\mu_{x,s}, \sigma_{x,s}^2\}$ .

##### A. Soft BA-MAP: Soft-Belief Mixture MAP-LLR Detector

We perform symbol-wise MAP detection using the full state uncertainty. The receiver maintains a soft belief (forward state distribution) and forms the per-symbol log-likelihood ratio (LLR) via belief-weighted Gaussian mixtures:

$$\Lambda_t(y) = \log \frac{p_1 \sum_s \alpha_t(s) f(y | x=1, s)}{p_0 \sum_s \alpha_t(s) f(y | x=0, s)} \quad (7)$$

$$= \log \frac{p_1 \sum_s \alpha_t(s) \mathcal{N}(y; \mu_{1,s}, \sigma_{1,s}^2)}{p_0 \sum_s \alpha_t(s) \mathcal{N}(y; \mu_{0,s}, \sigma_{0,s}^2)}.$$

The decision is formulated as  $\hat{X}_t = \mathbf{1}\{\Lambda_t(Y_t) > 0\}$ , which minimizes instantaneous bit error under the assumed model that considers ISI and the full mixtures.

##### B. BA-MAP: Belief-Adaptive MAP Thresholding

To obtain a lightweight decoding mechanism, we replace the full mixtures in (7) by belief-matched surrogates. From the current belief  $\alpha_t$ , compute the mixture moments

$$\mu_x^{\text{mix}} = \sum_s \alpha_t(s) \mu_{x,s}, \quad (8)$$

$$(\sigma_x^{\text{mix}})^2 = \sum_s \alpha_t(s) (\sigma_{x,s}^2 + \mu_{x,s}^2) - (\mu_x^{\text{mix}})^2 \quad (9)$$

where  $x \in \{0, 1\}$ . This method treats  $Y_t$  as drawn from two Gaussians with these moments and selects the per-symbol threshold  $\tau_t$  by the MAP condition

$$p_0 \mathcal{N}(\tau_t; \mu_0^{\text{mix}}, (\sigma_0^{\text{mix}})^2) = p_1 \mathcal{N}(\tau_t; \mu_1^{\text{mix}}, (\sigma_1^{\text{mix}})^2). \quad (10)$$

For equal variances,  $\tau_t$  in (10) yields the closed form

$$\tau_t = \frac{1}{2} (\mu_0^{\text{mix}} + \mu_1^{\text{mix}}) + \frac{(\sigma^{\text{mix}})^2}{\mu_1^{\text{mix}} - \mu_0^{\text{mix}}} \log \frac{p_0}{p_1},$$

otherwise it reduces to a quadratic form with two real roots; we select the root closest to their midpoint. Although replacing the belief-weighted Gaussian mixture with a single moment-matched Gaussian introduces approximation error, it remains accurate in two regimes: when ISI is weak, and when the belief concentrates on states with similar means/variances, so the mixture is effectively near-Gaussian. This approximation holds in most operating conditions; however, for small  $T_s$  ISI is strong and the belief can spread across dissimilar states, producing a strongly multimodal mixture. Consequently, BA-MAP can underperform Soft BA-MAP in this regime, as observed in Section V.

#### V. COMPUTATIONAL COMPLEXITY AND PERFORMANCE EVALUATION

We briefly analyze the per-symbol computational complexity of the proposed detectors. For an ISI memory order of  $m$ , the number of possible ISI states is  $2^m$ . In Soft BA-MAP, each symbol decision requires evaluating two belief-weighted Gaussian mixtures, corresponding to  $x = 0$  and  $x = 1$ . This results in  $\mathcal{O}(2^m)$  Gaussian likelihood evaluations per symbol, along with a belief update that also scales as  $\mathcal{O}(2^m)$ . For BA-MAP, the computation of belief-matched mixture moments and the subsequent solution of a scalar MAP threshold equation similarly require  $\mathcal{O}(2^m)$  operations per symbol. However, BA-MAP has significantly lower constant factors than Soft BA-MAP, since it avoids explicit mixture likelihood evaluations.

In terms of memory requirements, both methods maintain the forward state belief vector, which requires  $\mathcal{O}(2^m)$  memory. When the ISI memory order  $m$  is not too large ( $T_s$  values that are not extremely small), the diffusive channel response can be accurately captured with a limited number of states. In our study, we experimented with  $m$  values between 5 and 15. Under these conditions, the resulting memory and time constraints remain feasible. For typical MCvD parameters, the

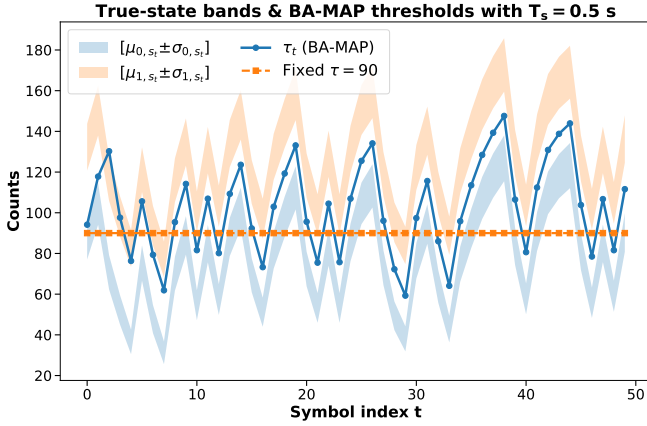


Fig. 2. Evolution of true-state Gaussian bands and adaptive thresholds for  $N_{Tx} = 1000$  over 50 symbols. Shaded regions show the true-state means with  $\pm 1\sigma$  intervals for bit-0 and bit-1. Solid circular markers indicate the belief-adaptive MAP thresholds (BA-MAP); square markers show a fixed threshold at  $\tau = 90$ . The point transmitter is located  $12.5\mu\text{m}$  from the center of a spherical receiver of radius  $5\mu\text{m}$ , with diffusion coefficient  $D = 79.4 \frac{\mu\text{m}^2}{\text{s}}$ .

ISI memory order  $m$  remains small (e.g.,  $m \leq 10$ ), which keeps the belief update and per-symbol detection computationally feasible in practice. If the decoder capabilities are further limited, smaller  $m$  values can be chosen for the system.

We benchmark proposed state-aware signal detectors against standard equalization and thresholding approaches commonly used in MCvD. The set of baselines includes Fixed Threshold detection, MMSE equalization (receiver-side), and PA (transmitter-side). Fixed Threshold applies a single decision boundary regardless of ISI history. MMSE is a linear receiver-side equalizer that reduces effective ISI prior to thresholding. In contrast, PA is a transmitter-side scheme that changes the emitted molecule count to mitigate average ISI, but it does not incorporate state-dependent noise into the detection rule.

Figure 2 illustrates the BA-MAP, our state-dependent thresholding mechanism, in a short symbol duration regime. The shaded regions denote the true-state molecule count distributions within one standard deviation around the mean for bit-0 and bit-1 under the current ISI state. In this regime, the received signal power fluctuates rapidly, making a fixed threshold inadequate: the horizontal decision line often falls outside the optimal separation region between the two symbol distributions. In contrast, the BA-MAP thresholds adapt to each ISI state by aligning with the belief-matched Gaussian statistics at every symbol (i.e., remaining between the  $\mu_0$  and  $\mu_1$  bands). This adaptivity significantly reduces the error probability compared to a fixed threshold detector.

Figure 3 compares the bit error rates (BER) of different decoding strategies for varying symbol durations and  $N^{Tx}$  values. At short symbol durations, heavy interference dominates, and all methods exhibit higher error rates. Among the methods, Soft BA-MAP achieves the lowest error rates across the entire range, since it directly incorporates state-dependent mean and variance through mixture likelihoods. BA-MAP and MMSE also provide significant improvements for reliability over other methods while maintaining low complexity. Although the BER curves in Figure 3 demonstrate the reliability advantages of our

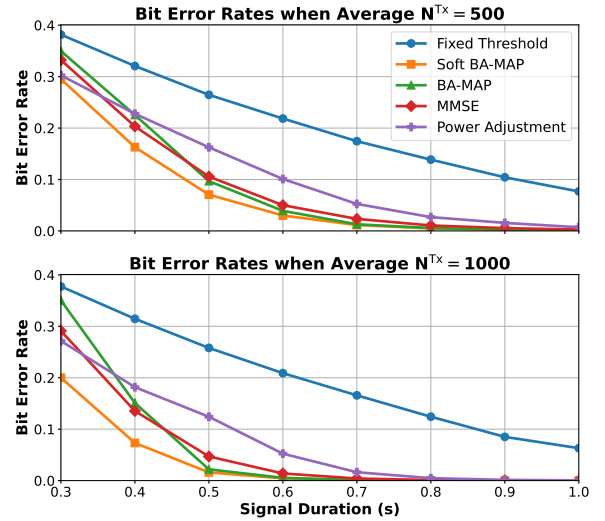


Fig. 3. Bit Error Rate (BER) performance of different decoding and equalization strategies, using the same system parameters as in Fig. 2.

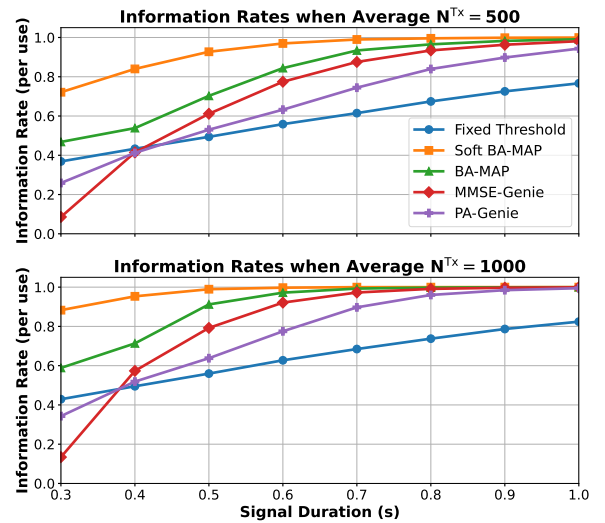


Fig. 4. Maximum achievable information rates of proposed methodologies with respect to  $T_s$ , using the same system parameters as in Fig. 2.

method over conventional equalization methods, BER alone does not fully capture the true performance of information transfer.

In contrast, the rate analysis directly quantifies how much information can be reliably communicated per channel use [17]. From this perspective, Figure 4 shows the superiority of our proposed methods. In this evaluation, information rates are calculated with genie-aided versions of MMSE and PA. In Genie-MMSE, the equalizer is assumed to know the true ISI state, and per-state MAP thresholds are computed in the MMSE output domain. For Genie-PA, the transmitter adjusts its emissions using the true residual interference from past states, and the receiver decodes with a fixed threshold. Both methods thus yield conditional rates  $I(X; \hat{Y} | S)$ , which serve as upper bounds for  $I(X; \hat{Y})$ . This upper-boundedness follows directly from the chain rule with i.i.d. inputs, since revealing

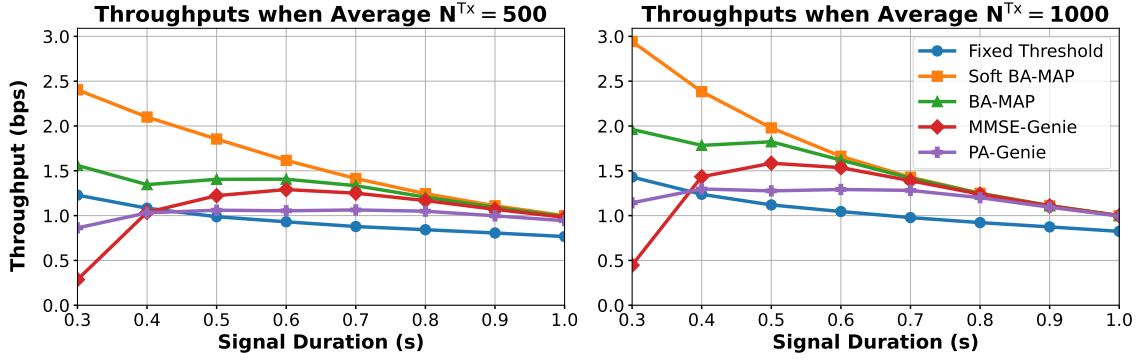


Fig. 5. Maximum achievable throughputs of proposed methodologies with respect to  $T_s$ , using the same system parameters as in Fig. 2.

the state  $S$  cannot decrease the mutual information.

Even without using state knowledge, Soft BA-MAP achieves up to a twofold increase in the information rate under practical parameter regimes compared to Genie-MMSE for practical symbol durations, and BA-MAP closely follows while maintaining low complexity. Fixed-threshold and Genie-PA, despite using optimized thresholds via sweeping, remain fundamentally limited. For short  $T_s$ ,  $h_0$  is very low and ISI dominates; a tuned fixed threshold leverages the residual count bias without inversion. By contrast, PA can further shrink  $h_0$  (hurting SNR), while MMSE's ill-conditioned ISI inversion at short  $T_s$  amplifies noise before a state-agnostic decision, so both underperform the fixed threshold technique in this region.

Similarly, Figure 5 captures the trade-off between symbol duration and transmission speed, showing that Soft BA-MAP consistently maximizes throughput and delivers almost twofold improvements in throughput.

## VI. CONCLUSION

This letter proposed two variance-aware detectors, Soft BA-MAP and BA-MAP, for molecular communication channels impaired by inter-symbol interference (ISI) and heteroscedastic noise. Both methods explicitly modeled the state-dependent mean and variance of the received molecule counts. Soft BA-MAP leveraged belief-weighted mixture likelihoods to perform symbol detection without relying on fixed scalar thresholds, while BA-MAP approximated these mixtures as single Gaussians to determine adaptive per-symbol MAP thresholds. Numerical results demonstrated that the proposed methods consistently outperformed classical equalization techniques by reducing bit error rates and enhancing information rates across various symbol durations. In particular, Soft BA-MAP achieved up to a twofold increase in throughput under practical parameter regimes compared to Genie-aided MMSE detection, highlighting the importance of explicitly accounting for state-dependent noise in molecular communication receivers. Future work will extend the proposed methods to multiple-input multiple-output (MIMO) scenarios [18], [19].

## REFERENCES

[1] N. Farsad, H. B. Yilmaz, A. Eckford, C.-B. Chae, and W. Guo, "A comprehensive survey of recent advancements in molecular communication," *IEEE Commun. Surveys Tuts.*, vol. 18, no. 3, pp. 1887–1919, 2016.

[2] C. Lee, B.-H. Koo, C.-B. Chae, and R. Schober, "The Internet of bio-nano things in blood vessels: System design and prototypes," *IEEE Trans. NanoBioscience*, vol. 25, no. 2, pp. 222–231, April 2023.

[3] V. Jamali, A. Ahmadzadeh, W. Wicke, A. Noel, and R. Schober, "Channel modeling for diffusive molecular communication—a tutorial review," *Proceedings of the IEEE*, vol. 107, no. 7, pp. 1256–1301, 2019.

[4] M. Ş. Kuran, H. B. Yilmaz, I. Demirkol, N. Farsad, and A. Goldsmith, "A survey on modulation techniques in molecular communication via diffusion," *IEEE Commun. Surveys Tuts.*, vol. 23, no. 1, pp. 7–28, 2020.

[5] S. Pudasaini, S. Shin, and K. S. Kwak, "Robust modulation technique for diffusion-based molecular communication in nanonetworks," *arXiv preprint arXiv:1401.3938*, 2014.

[6] M. J. Hautus, N. A. Macmillan, and C. D. Creelman, *Detection theory: A user's guide*. Routledge, 2021.

[7] H. B. Yilmaz and C.-B. Chae, "Arrival modelling for molecular communication via diffusion," *Elec. Lett.*, vol. 50, no. 23, pp. 1667–1669, 2014.

[8] M. Damrath, S. Korte, and P. A. Hoeher, "Equivalent discrete-time channel modeling for molecular communication with emphasize on an absorbing receiver," *IEEE Trans. Nanobioscience*, vol. 16, no. 1, pp. 60–68, 2017.

[9] B. Tepekule, A. E. Pusane, H. B. Yilmaz, C.-B. Chae, and T. Tugcu, "ISI mitigation techniques in molecular communication," *IEEE Trans. Mol. Biol. Multi-Scale Commun.*, vol. 1, no. 2, pp. 202–216, 2015.

[10] D. Kilinc and O. B. Akan, "Receiver design for molecular communication," *IEEE J. Sel. Areas Commun.*, vol. 31, no. 12, pp. 705–714, 2014.

[11] G. D. Forney, "The Viterbi algorithm," *Proc. IEEE*, vol. 61, no. 3, pp. 268–278, 2005.

[12] M. S. Thakur, S. Sharma, and V. Bhatia, "Iterative signal detection to mitigate isi and mui for diffusion-based molecular communications," *Nano Communication Networks*, vol. 30, p. 100377, 2021.

[13] G. Genç, "Reception modeling and achievable rate analysis of sphere-to-sphere molecular communication via diffusion," 2018.

[14] G. Genç, Y. E. Kara, H. B. Yilmaz, and T. Tugcu, "ISI-aware modeling and achievable rate analysis of the diffusion channel," *IEEE Commun. Lett.*, vol. 20, no. 9, pp. 1729–1732, 2016.

[15] S. Verdú *et al.*, "A general formula for channel capacity," *IEEE Trans. Inf. Theory*, vol. 40, no. 4, pp. 1147–1157, 1994.

[16] D.-M. Arnold, H.-A. Loeliger, P. O. Vontobel, A. Kavcic, and W. Zeng, "Simulation-based computation of information rates for channels with memory," *IEEE Trans. Inf. Theory*, vol. 52, no. 8, pp. 3498–3508, 2006.

[17] Y.-P. Hsieh and P.-C. Yeh, "Mathematical foundations for information theory in diffusion-based molecular communications," *arXiv preprint arXiv:1311.4431*, 2013.

[18] B.-H. Koo, C. Lee, H. B. Yilmaz, N. Farsad, A. Eckford, and C.-B. Chae, "Molecular MIMO: From theory to prototype," *IEEE Journal on Selected Areas in Communications*, vol. 34, no. 3, pp. 600–614, 2016.

[19] B.-H. Koo, C. Lee, A. E. Pusane, T. Tugcu, and C.-B. Chae, "MIMO operations in molecular communications: Theory, prototypes, and open challenges," *IEEE Communications Magazine*, vol. 59, no. 9, pp. 98–104, 2021.